Control of neuronal excitation-inhibition balance by BMP-SMAD1 signaling

Zeynep Okur[1], Nadia Schlauri[1,†], Vassilis Bitsikas[1], Myrto Panopoulou[1], Kajari Karmakar[1, ††], Dietmar Schreiner[1], Peter Scheiffele[1*]

[1]Biozentrum, University of Basel, Spitalstrasse 41, CH-4056, Basel, Switzerland

[†]present address: Department of Biomedicine, University of Basel, Hebelstrasse 20, 4053 Basel, Switzerland

[††]present address: Roche Pharmaceutical Research and Early Development, Roche Innovation Center Basel, Grenzacherstr. 124, 4070 Basel, Switzerland

*Corresponding author: peter.scheiffele@unibas.ch

Summary

Throughout life, neuronal networks in the mammalian neocortex maintain a balance of excitation and inhibition which is essential for neuronal computation. Deviations from a balanced state have been linked to neurodevelopmental disorders and severe disruptions result in epilepsy. To maintain balance, neuronal microcircuits composed of excitatory and inhibitory neurons sense alterations in neural activity and adjust neuronal connectivity and function. Here, we identified a signaling pathway in the adult mouse neocortex that is activated in response to elevated neuronal network activity. Over-activation of excitatory neurons is signaled to the network through the elevation of BMP2, a growth factor well-known for its role as morphogen in embryonic development. BMP2 acts on parvalbumin-expressing (PV) interneurons through the transcription factor SMAD1, which controls an array of glutamatergic synapse proteins and components of peri-neuronal nets. PV interneuron-specific impairment of BMP2-SMAD1 signaling is accompanied by a loss of PV cell glutamatergic innervation, underdeveloped peri-neuronal nets, and decreased excitability. Ultimately, this impairment of PV interneuron functional recruitment disrupts cortical excitation – inhibition balance with mice exhibiting spontaneous epileptic seizures. Our findings suggest that developmental morphogen signaling is re-purposed to stabilize cortical networks in the adult mammalian brain.

Introduction

Neuronal circuits in the neocortex underlie our ability to perceive our surroundings, integrate various forms of sensory information, and support cognitive functions. Cortical computation

relies on assemblies of excitatory and inhibitory neuron types that are joined into canonical microcircuit motifs. The synaptic innervation and intrinsic properties of fast-spiking parvalbumin-expressing inhibitory interneurons (PV interneurons) have emerged as key parameters for controlling cortical circuit stability and plasticity [1,2]. During development, sensory experience shapes synaptic innervation of PV interneurons in an afferent-specific manner and synaptic input to PV interneuron dendrites is a critical node for cortical dysfunction in neurodevelopmental disorders [3-7]. In the adult brain, neuronal activity-dependent regulation of PV interneuron recruitment and excitability are fundamental for the maintenance of excitation – inhibition balance and have been implicated in gating cortical circuit plasticity during learning processes [2,8-12]. However, the molecular mechanisms underlying these critical features, in particular trans-cellular signaling events that relay alterations in neuronal network activity and adjust PV interneuron function are poorly understood.

Bone Morphogenetic Protein signaling is mobilized by neuronal network activity in adult neocortex

To identify candidate trans-cellular signals that are regulated by neuronal network activity in mature neocortical neurons, we examined secreted growth factors of the bone morphogenetic protein family (BMPs), which had been implicated in cell fate specification and neuronal growth during development [13-20]. Amongst four bone morphogenetic proteins (BMP2,4,6,7) examined, *Bmp2* mRNA was significantly upregulated in glutamatergic neurons upon stimulation (3.5 +/- 0.5 fold, Extended Data Fig. 1a-d). A similar activity-dependent elevation of BMP2 was observed at the protein level in neurons derived from a *Bmp2* HA-tag knock-in mouse (*Bmp2*$^{HA/HA}$, Extended Data Fig. 1e-g). BMPs are well known for their function as developmental morphogens and in fate specification of neuronal progenitors, where they direct gene regulation in recipient cells through SMAD transcription factors (Fig. 1a) [21-26]. Interestingly, the canonical BMP- target genes *Id1* and *Smad6* were significantly upregulated in stimulated neocortical cultures, a process that was blocked by addition of the extracellular BMP-antagonist Noggin (Extended Data Fig. 1h, i). In the neocortex of adult mice, key BMP signaling components continue to be expressed with the ligand BMP2 exhibiting highest mRNA levels in glutamatergic neurons (Extended Data Fig. 2a-c). To test whether BMP-target gene transcription is activated in response to elevated neuronal network activity in adult mice, we chemogenetically silenced upper layer PV interneurons in the barrel cortex (Fig. 1b). This local reduction of PV neuron-mediated inhibition results in increased neuronal network activity [27,28] accompanied by a 4- to 8-fold transcript increase for the activity-induced primary response

genes *cfos* and *Bdnf* (Fig. 1c). Importantly, this chemogenetic stimulation also resulted in upregulation of four critical SMAD1/5-dependent BMP target genes (*Id1*, *Id3*, *Smad6* and *Smad7*) (Fig. 1c). To monitor BMP target gene activation with temporal and cell type-specific resolution *in vivo*, we developed a novel temporally-controlled BMP-signaling reporter (Fig. 1d). We combined BMP-response element sequences (4xBRE) from the *Id1* promoter [29] with the small molecule (LMI070)-gated miniX^{on} cassette [30] to drive a nucleus-targeted eGFP (Extended Data Fig. 3a). Thus, the level of nuclear eGFP reports activation of BMP-signaling during a time window specified by LMI070 application (Extended Data Fig 3a-c). Notably, chemogenetic stimulation in presence of LMI070 resulted in a 3-fold increase in eGFP intensity in PV interneurons (Fig. 1e-g). In aggregate, these results demonstrate that increased cortical network activity mobilizes BMP2 signaling to alter transcriptional responses in PV interneurons in the adult mouse barrel cortex.

BMP-SMAD1 signaling controls transcriptional regulation of synaptic proteins

During development, the combinatorial action of various BMP ligands and receptors directs cell type-specific target gene regulation through SMAD transcription factors, but also SMAD-independent functions have been described [13,15,17,19,31-36]. In neocortical neurons, BMP2 stimulation (20 ng/ml for 45 minutes) resulted in SMAD1/5 activation in both, glutamatergic and GABAergic neurons (Extended Data Fig. 4a-c). To uncover SMAD1 target genes in postmitotic mammalian neurons, we performed chromatin immunoprecipitation sequencing (ChiP-seq) for Smad1/5 from naïve and BMP2-stimulated neocortical cultures (Fig. 2a). We found 349 BMP2-responsive (> 2-fold increase and p.adj value < 0.05) SMAD1/5 binding sites and 167 sites that were bound constitutively (stimulation independent, < 2-fold increase and p.adj value< 0.05) (Fig. 2b and Supplementary Table 1). Importantly, BMP2-responsive peaks were associated with promoter elements whereas the majority of constitutive SMAD1/5 binding regions were promoter-distal. To explore whether SMAD1 triggers *de novo* activation of target genes or rather modifies transcriptional output of active genes, we mapped active regulatory elements by performing ChiP-seq for histone 3 acetylated at lysine 27 (H3K27ac), a chromatin modification that marks active promoters and enhancers. By intersecting H3K27ac ChiP-seq signals with SMAD1/5 peaks (Fig. 2b-e), we found that the majority of BMP2-responsive regulatory elements are already active in naïve cultures. By comparison, constitutively bound regions exhibited only low H3K27ac signal (Fig. 2b, c) suggesting that they are transcriptionally silent. Sequence analysis confirmed enrichment of the SMAD1/5 DNA binding motif in the BMP2-responsive gene regulatory elements (Fig. 2d). The impact of BMP2-induced SMAD1/5 recruitment on transcriptional output was examined by RNA-

sequencing (Fig. 2a). Differential gene expression analysis identified 30 and 147 up-regulated transcripts 1 and 6 hours after BMP2-stimulation, respectively (Extended Data Fig. 4c, Supplementary Table 2). 50% of the regulated genes 1 hour after BMP2-stimulation had direct Smad1/5 binding at their promoters and included negative feedback loop genes of the BMP signaling pathway (*Id1*, *Id3* and *Smad7*). 25% of differentially regulated genes 6 hours after BMP2-stimulation had direct Smad1/5 binding. (Extended Data Fig. 4d). Conditional knock-out of *Smad1* in post-mitotic neurons was sufficient to abolish upregulation of these genes in response to BMP2 signaling and reduced their expression in naïve (unstimulated) neurons (Fig. 2f and Extended Data Fig. 4e,f Supplementary Table 3). Direct transcriptional targets of BMP-SMAD1 signaling in neocortical neurons included an array of activity-regulated genes such as *Junb*, *Trib1* and *Pim3*, key components of the extracellular matrix (*Bcan, Gpc6*) and glutamatergic synapses (*Lrrc4*, *Grin3a*) (Fig.2e, Extended Data Fig. 4d). Moreover, neuronal *Smad1* ablation was accompanied by broad gene expression changes beyond de-regulation of direct SMAD1 target genes (Fig. 2g). Top GO terms enriched amongst the upregulated genes were “glutamatergic synapse” and transcription factors under the term “nucleus” (Fig. 2h). Furthermore, de-regulated genes include the majority of neuronal activity-regulated rapid primary (rPRG) and secondary (SRG) activity-response genes (Fig. 2i). Thus, SMAD1 is the key downstream mediator of BMP signaling in mature neurons and its neuronal loss of function results in a severe imbalance of neuronal network activity *in vitro*.

Synaptic innervation and excitability of PV interneurons are controlled by SMAD1

PV interneurons in neocortical circuits are key regulators of excitation – inhibition balance and glutamatergic synapse formation onto PV interneurons and peri-neuronal nets (PNNs) surrounding these cells are modified in response to changes in neuronal network activity [37,38]. To test whether SMAD1 regulates synapse formation onto PV interneurons, we generated conditional *Smad1* knock-out mice. Postnatal ablation of *Smad1* in PV interneurons ($PV^{cre/+}$::$Smad1^{fl/fl}$; $Smad1^{\Delta PV}$ mice) did not alter PV cell density or distribution in the somatosensory cortex of adult mice (Extended Data Fig. 5a-c). We then adopted genetically encoded intrabodies (Fibronectin intrabodies generated by mRNA display, FingRs) directed against PSD-95 and gephyrin (GEPH) to quantitatively map synaptic inputs to PV interneurons *in vivo* [39] (Extended Data Fig. 6a-c). FingR probes were selectively expressed in PV interneurons in layer 2/3 of barrel cortex using cre recombinase-dependent adeno-associated viruses (Fig. 3a-g, Extended Data Fig. 6a-c and Supplementary Movie 1). In $Smad1^{\Delta PV}$ mice, we observed a 40% reduction in morphological glutamatergic synapse density onto PV interneurons (Fig. 3b, c). This was accompanied by a comparable reduction in mEPSC frequency but no change in mEPSC amplitude in acute slice recordings (Fig. 3d-f). The density

of peri-somatic PV-PV synapses (identified by synaptotagmin-2 and FingR GPHN co-localization) was also reduced (Fig. 3h, i), but there was no significant change in mIPSC frequency or amplitude in PV cells of *Smad1*$^{\Delta PV}$ mice, likely due to compensatory inhibition derived from other interneuron classes (Fig. 3j-l). Thus, SMAD1 is required for normal functional glutamatergic innervation of layer 2/3 PV interneurons, resulting in reduced glutamatergic input to these cells in *Smad1*$^{\Delta PV}$ mice.

Neuronal activity-induced regulation in PV interneurons modifies the elaboration of PNNs and parvalbumin expression [1,27,37,38,40,41], and our ChiP-Seq analysis identified the PNN component brevican (*Bcan*) as one of the direct SMAD1 targets in neuronal cells. In *Smad1*$^{\Delta PV}$ mice, the elaboration of PNNs around PV interneurons and parvalbumin protein expression were significantly reduced (Fig. 4a-c). This results in a significant reduction in the density of parvalbumin-immuno-reactive cells in layer 2/3, despite the normal density of genetically-defined PV interneurons (Extended Data Fig. 5a-c). Through organizing PNNs, Brevican has been implicated in regulating plasticity and excitability of PV interneurons [38]. Interestingly, the firing rate of SMAD1-deficient PV interneurons in response to current injections was significantly reduced in the barrel cortex of adult mice (Fig. 4d-f and Extended Data Fig. 5d, note that firing rate was unchanged in young animals, Extended Data Fig. 5e). This reduced firing frequency most likely is explained by a reduction in input resistance in the *Smad1*$^{\Delta PV}$ cells (Extended Data Fig. 5d). Thus, in the absence of BMP-SMAD1 signaling PV interneurons not only receive less glutamatergic drive but are also less excitable. These cellular alterations resulted in a severe overall disruption of cortical excitation – inhibition balance. As compared to control littermates, *Smad1*$^{\Delta PV}$ mice exhibited hyperactivity in open field tests and frequently exhibited spontaneous seizures when introduced into novel environments (Fig. 4g, h). Video-coupled EEG recordings with electrodes over the barrel cortex (Supplementary Movie 2) revealed marked high amplitude activity bursts at the time of seizure followed by a refractory period (Fig. 4i). Overall, our results demonstrate that elevated network activity in the somatosensory cortex of adult mice triggers the upregulation of BMP2 in glutamatergic neurons which balances excitation by controlling synaptic innervation and function of PV interneurons through the transcriptional factor SMAD1.

Discussion

Despite being exposed to a wide range of sensory stimulus intensities, cortical circuits exhibit remarkably stable activity patterns that enable optimal information coding by the network. This network stability is achieved by homeostatic adaptations that modify the excitability of

individual neurons, scale the strength of synapses, as well as microcircuit-wide modifications of excitatory and inhibitory synapse density [10,12,42-45]. These multiple adaptations occur at various time-scales, from near instantaneous adjustments of excitation and inhibition during sensory processing [46], to slower modifications of synaptic connectivity upon longer-term shifts in circuit activation as they occur during sensory deprivation but also in disease states [12,47-51]. Thus, both rapid cell intrinsic, as well as long-lasting trans-cellular signaling processes have evolved to ensure cortical network function and stability.

Differential recruitment of PV interneuron-mediated inhibition has emerged as a key node for the control of excitation – inhibition balance and cortical plasticity [2,8,9]. We here demonstrate that elevated neuronal network activity in the somatosensory cortex of adult mice triggers BMP target gene expression in PV interneurons. The transcription factor SMAD1, directly binds to and regulates promoters of an array of glutamatergic synapse proteins and components of the perineuronal nets, such as brevican. Thus, BMP2-SMAD signaling provides a trans-neuronal signal to adjust functional PV interneuron recruitment and excitability that ultimately serve to maintain excitation – inhibition balance and stabilize cortical network function in adult neocortex. In developing auditory cortex, genetic deletion of type I BMP-receptors from PV interneurons is associated with a loss of spike-timing dependent LTP at PV interneuron output synapses onto principal neurons of layer 4 whereas basal GABAergic transmission was unchanged [52]. This suggests a selective role for BMP2-SMAD1 signaling in controlling glutamatergic input connectivity to PV interneurons.

Importantly, transcriptional regulation through BMP2-SMAD1 signaling significantly differs from the action of activity-induced immediate early genes. As secreted growth factor, BMP2 derived from glutamatergic neurons relays elevated network activity to PV interneurons through the activation of an array of SMAD1 target genes. Rather than ON/OFF responses, the majority of direct SMAD1 targets exhibit active enhancer and promoter elements and are already expressed under basal conditions. However, SMAD1 activation results in an elevation of transcriptional output, indicating a graded gene expression response to BMP2.

In early development, BMP growth factors act as morphogens that carry positional information and differentially instruct cell fates [23,24,26]. The combinatorial complexity arising from the substantial number of BMP ligands and receptors has the power to encode computations for finely tuned cell-type-specific responses [32,53]. Our work suggests that the spatiotemporal coding power, robustness, and flexibility which evolved for developmental patterning is harnessed for balancing plasticity and stability of neuronal circuits in the adult mammalian brain. Notably, additional BMP ligands besides BMP2 are selectively expressed in neocortical cell types (Extended Data Fig. 2b). Moreover, an array of type I and type II BMP receptors are

detected across neocortical cell populations. This suggests that BMP-signaling might control additional aspects of cell-cell communication in the mammalian neocortex.

Disruptions in excitation – inhibition balance and homeostatic adaptations have been implicated in neurodevelopmental disorders as there is reduced GABAergic signaling and a propensity to develop epilepsy in individuals with autism [49-51,54]. Considering that BMP-signaling pathways can be targeted with peptide mimetics [55] they may provide an entry point for therapeutic interventions in neurodevelopmental disorders characterized by disruptions in PV interneuron innervation, excitation – inhibition balance, and seizures.

References and notes:

1 Dehorter, N. *et al.* Tuning of fast-spiking interneuron properties by an activity-dependent transcriptional switch. *Science (New York, N.Y* **349**, 1216-1220 (2015). https://doi.org:10.1126/science.aab3415

2 Takesian, A. E. & Hensch, T. K. Balancing plasticity/stability across brain development. *Prog Brain Res* **207**, 3-34 (2013). https://doi.org:10.1016/B978-0-444-63327-9.00001-1

3 Fazzari, P. *et al.* Control of cortical GABA circuitry development by Nrg1 and ErbB4 signalling. *Nature* **464**, 1376-1380 (2010). https://doi.org:10.1038/nature08928

4 Sun, Y. *et al.* Neuregulin-1/ErbB4 Signaling Regulates Visual Cortical Plasticity. *Neuron* **92**, 160-173 (2016). https://doi.org:10.1016/j.neuron.2016.08.033

5 Pouchelon, G. *et al.* The organization and development of cortical interneuron presynaptic circuits are area specific. *Cell reports* **37**, 109993 (2021). https://doi.org:10.1016/j.celrep.2021.109993

6 Bernard, C. *et al.* Cortical wiring by synapse type-specific control of local protein synthesis. *Science (New York, N.Y* **378**, eabm7466 (2022). https://doi.org:10.1126/science.abm7466

7 Pelkey, K. A. *et al.* Pentraxins coordinate excitatory synapse maturation and circuit integration of parvalbumin interneurons. *Neuron* **85**, 1257-1272 (2015). https://doi.org:10.1016/j.neuron.2015.02.020

8 Xue, M., Atallah, B. V. & Scanziani, M. Equalizing excitation-inhibition ratios across visual cortical neurons. *Nature* **511**, 596-600 (2014). https://doi.org:10.1038/nature13321

9 Zhou, M. *et al.* Scaling down of balanced excitation and inhibition by active behavioral states in auditory cortex. *Nature neuroscience* **17**, 841-850 (2014). https://doi.org:10.1038/nn.3701

10 Froemke, R. C. Plasticity of cortical excitatory-inhibitory balance. *Annu Rev Neurosci* **38**, 195-219 (2015). https://doi.org:10.1146/annurev-neuro-071714-034002

11 Yap, E. L. *et al.* Bidirectional perisomatic inhibitory plasticity of a Fos neuronal network. *Nature* **590**, 115-121 (2021). https://doi.org:10.1038/s41586-020-3031-0

12 Spiegel, I. *et al.* Npas4 regulates excitatory-inhibitory balance within neural circuits through cell-type-specific gene programs. *Cell* **157**, 1216-1229 (2014). https://doi.org:10.1016/j.cell.2014.03.058

13 McCabe, B. D. *et al.* The BMP homolog Gbb provides a retrograde signal that regulates synaptic growth at the Drosophila neuromuscular junction. *Neuron* **39**, 241-254 (2003).

14 Marques, G. *et al.* The Drosophila BMP type II receptor Wishful Thinking regulates neuromuscular synapse morphology and function. *Neuron* **33**, 529-543 (2002). https://doi.org:S0896627302005950 [pii]

15 Ting, C. Y. *et al.* Tiling of r7 axons in the Drosophila visual system is mediated both by transduction of an activin signal to the nucleus and by mutual repulsion. *Neuron* **56**, 793-806 (2007). https://doi.org:10.1016/j.neuron.2007.09.033
16 Keshishian, H. & Kim, Y. S. Orchestrating development and function: retrograde BMP signaling in the Drosophila nervous system. *Trends in neurosciences* **27**, 143-147 (2004).
17 Kalinovsky, A. *et al.* Regulation of axon-target specificity of ponto-cerebellar afferents by BMP signaling. *PLoS Biol* **9**, e1001013 (2011).
18 Xiao, L. *et al.* BMP signaling specifies the development of a large and fast CNS synapse. *Nature neuroscience* **16**, 856-864 (2013). https://doi.org:10.1038/nn.3414
19 Higashi, T., Tanaka, S., Iida, T. & Okabe, S. Synapse Elimination Triggered by BMP4 Exocytosis and Presynaptic BMP Receptor Activation. *Cell reports* **22**, 919-929 (2018). https://doi.org:10.1016/j.celrep.2017.12.101
20 Aihara, S., Fujimoto, S., Sakaguchi, R. & Imai, T. BMPR-2 gates activity-dependent stabilization of primary dendrites during mitral cell remodeling. *Cell reports* **35**, 109276 (2021). https://doi.org:10.1016/j.celrep.2021.109276
21 Liem, K. F., Jr., Tremml, G. & Jessell, T. M. A role for the roof plate and its resident TGFbeta-related proteins in neuronal patterning in the dorsal spinal cord. *Cell* **91**, 127-138 (1997).
22 Shi, Y. & Massague, J. Mechanisms of TGF-beta signaling from cell membrane to the nucleus. *Cell* **113**, 685-700 (2003). https://doi.org:S009286740300432X [pii]
23 Hogan, B. L. Bone morphogenetic proteins in development. *Curr Opin Genet Dev* **6**, 432-438 (1996). https://doi.org:10.1016/s0959-437x(96)80064-5
24 De Robertis, E. M. & Kuroda, H. Dorsal-ventral patterning and neural induction in Xenopus embryos. *Annu Rev Cell Dev Biol* **20**, 285-308 (2004). https://doi.org:10.1146/annurev.cellbio.20.011403.154124
25 Rowitch, D. H. & Kriegstein, A. R. Developmental genetics of vertebrate glial-cell specification. *Nature* **468**, 214-222 (2010). https://doi.org:10.1038/nature09611
26 Mukhopadhyay, A., McGuire, T., Peng, C. Y. & Kessler, J. A. Differential effects of BMP signaling on parvalbumin and somatostatin interneuron differentiation. *Development (Cambridge, England)* **136**, 2633-2642 (2009). https://doi.org:10.1242/dev.034439
27 Devienne, G. *et al.* Regulation of perineuronal nets in the adult cortex by the activity of the cortical network. *J Neurosci* **41**, 5779-5790 (2021). https://doi.org:10.1523/JNEUROSCI.0434-21.2021
28 Goldenberg, A. M. *et al.* Localized chemogenetic silencing of inhibitory neurons: a novel mouse model of focal cortical epileptic activity. *Cereb Cortex* (2022). https://doi.org:10.1093/cercor/bhac245
29 Lewis, T. C. & Prywes, R. Serum regulation of Id1 expression by a BMP pathway and BMP responsive element. *Biochim Biophys Acta* **1829**, 1147-1159 (2013). https://doi.org:10.1016/j.bbagrm.2013.08.002
30 Monteys, A. M. *et al.* Regulated control of gene therapies by drug-induced splicing. *Nature* **596**, 291-295 (2021). https://doi.org:10.1038/s41586-021-03770-2
31 Massague, J. How cells read TGF-beta signals. *Nat Rev Mol Cell Biol* **1**, 169-178 (2000).
32 Su, C. J. *et al.* Ligand-receptor promiscuity enables cellular addressing. *Cell Syst* **13**, 408-425 e412 (2022). https://doi.org:10.1016/j.cels.2022.03.001
33 Butler, S. J. & Dodd, J. A role for BMP heterodimers in roof plate-mediated repulsion of commissural axons. *Neuron* **38**, 389-401 (2003).
34 Vicidomini, R. & Serpe, M. Local BMP signaling: A sensor for synaptic activity that balances synapse growth and function. *Curr Top Dev Biol* **150**, 211-254 (2022). https://doi.org:10.1016/bs.ctdb.2022.04.001
35 Eaton, B. A. & Davis, G. W. LIM Kinase1 Controls Synaptic Stability Downstream of the Type II BMP Receptor. *Neuron* **47**, 695-708 (2005).

36 Marques, G. *et al.* Retrograde Gbb signaling through the Bmp type 2 receptor wishful thinking regulates systemic FMRFa expression in Drosophila. *Development (Cambridge, England)* **130**, 5457-5470 (2003). https://doi.org:10.1242/dev.00772 dev.00772 [pii]
37 Li, K. X. *et al.* Neuregulin 1 regulates excitability of fast-spiking neurons through Kv1.1 and acts in epilepsy. *Nature neuroscience* **15**, 267-273 (2011). https://doi.org:10.1038/nn.3006
38 Favuzzi, E. *et al.* Activity-Dependent Gating of Parvalbumin Interneuron Function by the Perineuronal Net Protein Brevican. *Neuron* **95**, 639-655 e610 (2017). https://doi.org:10.1016/j.neuron.2017.06.028
39 Gross, G. G. *et al.* Recombinant probes for visualizing endogenous synaptic proteins in living neurons. *Neuron* **78**, 971-985 (2013). https://doi.org:10.1016/j.neuron.2013.04.017
40 Dehorter, N., Marichal, N., Marin, O. & Berninger, B. Tuning neural circuits by turning the interneuron knob. *Curr Opin Neurobiol* **42**, 144-151 (2017). https://doi.org:10.1016/j.conb.2016.12.009
41 Joseph, D. J. *et al.* Postnatal Arx transcriptional activity regulates functional properties of PV interneurons. *iScience* **24**, 101999 (2021). https://doi.org:10.1016/j.isci.2020.101999
42 Chen, L., Li, X., Tjia, M. & Thapliyal, S. Homeostatic plasticity and excitation-inhibition balance: The good, the bad, and the ugly. *Curr Opin Neurobiol* **75**, 102553 (2022). https://doi.org:10.1016/j.conb.2022.102553
43 Iascone, D. M. *et al.* Whole-Neuron Synaptic Mapping Reveals Spatially Precise Excitatory/Inhibitory Balance Limiting Dendritic and Somatic Spiking. *Neuron* **106**, 566-578 e568 (2020). https://doi.org:10.1016/j.neuron.2020.02.015
44 Marder, E. & Goaillard, J. M. Variability, compensation and homeostasis in neuron and network function. *Nat Rev Neurosci* **7**, 563-574 (2006). https://doi.org:10.1038/nrn1949
45 Turrigiano, G. G. & Nelson, S. B. Homeostatic plasticity in the developing nervous system. *Nat Rev Neurosci* **5**, 97-107 (2004).
46 Okun, M. & Lampl, I. Instantaneous correlation of excitation and inhibition during ongoing and sensory-evoked activities. *Nature neuroscience* **11**, 535-537 (2008). https://doi.org:10.1038/nn.2105
47 Keck, T. *et al.* Synaptic scaling and homeostatic plasticity in the mouse visual cortex in vivo. *Neuron* **80**, 327-334 (2013). https://doi.org:10.1016/j.neuron.2013.08.018
48 Mardinly, A. R. *et al.* Sensory experience regulates cortical inhibition by inducing IGF1 in VIP neurons. *Nature* **531**, 371-375 (2016). https://doi.org:10.1038/nature17187
49 Cellot, G. & Cherubini, E. GABAergic signaling as therapeutic target for autism spectrum disorders. *Front Pediatr* **2**, 70 (2014). https://doi.org:10.3389/fped.2014.00070
50 Rubenstein, J. L. & Merzenich, M. M. Model of autism: increased ratio of excitation/inhibition in key neural systems. *Genes Brain Behav* **2**, 255-267 (2003).
51 Nelson, S. B. & Valakh, V. Excitatory/Inhibitory Balance and Circuit Homeostasis in Autism Spectrum Disorders. *Neuron* **87**, 684-698 (2015). https://doi.org:10.1016/j.neuron.2015.07.033
52 Vickers, E. *et al.* LTP of inhibition at PV interneuron output synapses requires developmental BMP signaling. *Sci Rep* **10**, 10047 (2020). https://doi.org:10.1038/s41598-020-66862-5
53 Klumpe, H. E. *et al.* The context-dependent, combinatorial logic of BMP signaling. *Cell Syst* **13**, 388-407 e310 (2022). https://doi.org:10.1016/j.cels.2022.03.002
54 Exposito-Alonso, D. & Rico, B. Mechanisms Underlying Circuit Dysfunction in Neurodevelopmental Disorders. *Annu Rev Genet* **56**, 391-422 (2022). https://doi.org:10.1146/annurev-genet-072820-023642
55 Carlson, W. D., Keck, P. C., Bosukonda, D. & Carlson, F. R., Jr. A Process for the Design and Development of Novel Bone Morphogenetic Protein-7 (BMP-7) Mimetics

With an Example: THR-184. *Frontiers in pharmacology* **13**, 864509 (2022). https://doi.org:10.3389/fphar.2022.864509
56 Tyssowski, K. M. *et al.* Different Neuronal Activity Patterns Induce Different Gene Expression Programs. *Neuron* **98**, 530-546 e511 (2018). https://doi.org:10.1016/j.neuron.2018.04.001

Acknowledgements: We thank Özgür Genç, Zayna Chaker, Gustavo Aguilar, Wuzhou Yang, Josef Bischofberger, Ralf Schneggenburger and Kelly Tan for support, advice and valuable comments on the manuscript. Michaela Schwaiger for expert support in ChiP-seq analysis, Caroline Bornmann, Sabrina Innocenti, Enrique Perez-Garci for technical assistance. We are grateful to the Biozentrum Imaging Core Facility, the Centre for Transgenic Models, and the Quantitative Genomics facility Basel for expert technical support. This work was financially supported by a Fellowship of Excellence to Z.O., an EMBO Long-term Fellowship to M.P (ALTF 672-2022), and Grants from the Swiss National Science Foundation to P.S. (grant # 179432, # 154455, and # 209273). The Scheiffele Laboratory is an Associated member of the NCCR RNA & Disease.

Author contributions: All authors contributed to the design and analysis of experiments. Z.O. and N.S. conducted genetic and in vivo manipulations, Z.O. and M.P. conducted electrophysiological recordings, V.B. conducted EEG recordings, Z.O., D.S., N.S. and K.K. performed molecular biology procedures. Z.O. and P.S. wrote the manuscript.

Competing interests: The authors declare no competing interests.

Materials & correspondence: ChiP-seq and gene expression data will be deposited at GEO. All renewable reagents will be distributed by the corresponding author (peter.scheiffele@unibas.ch) or deposited in public repositories for distribution. The regulatory elements of the X^{on} system and cDNA sequences encoding FingRs will be distributed in accordance with respective MTAs.

Fig. 1

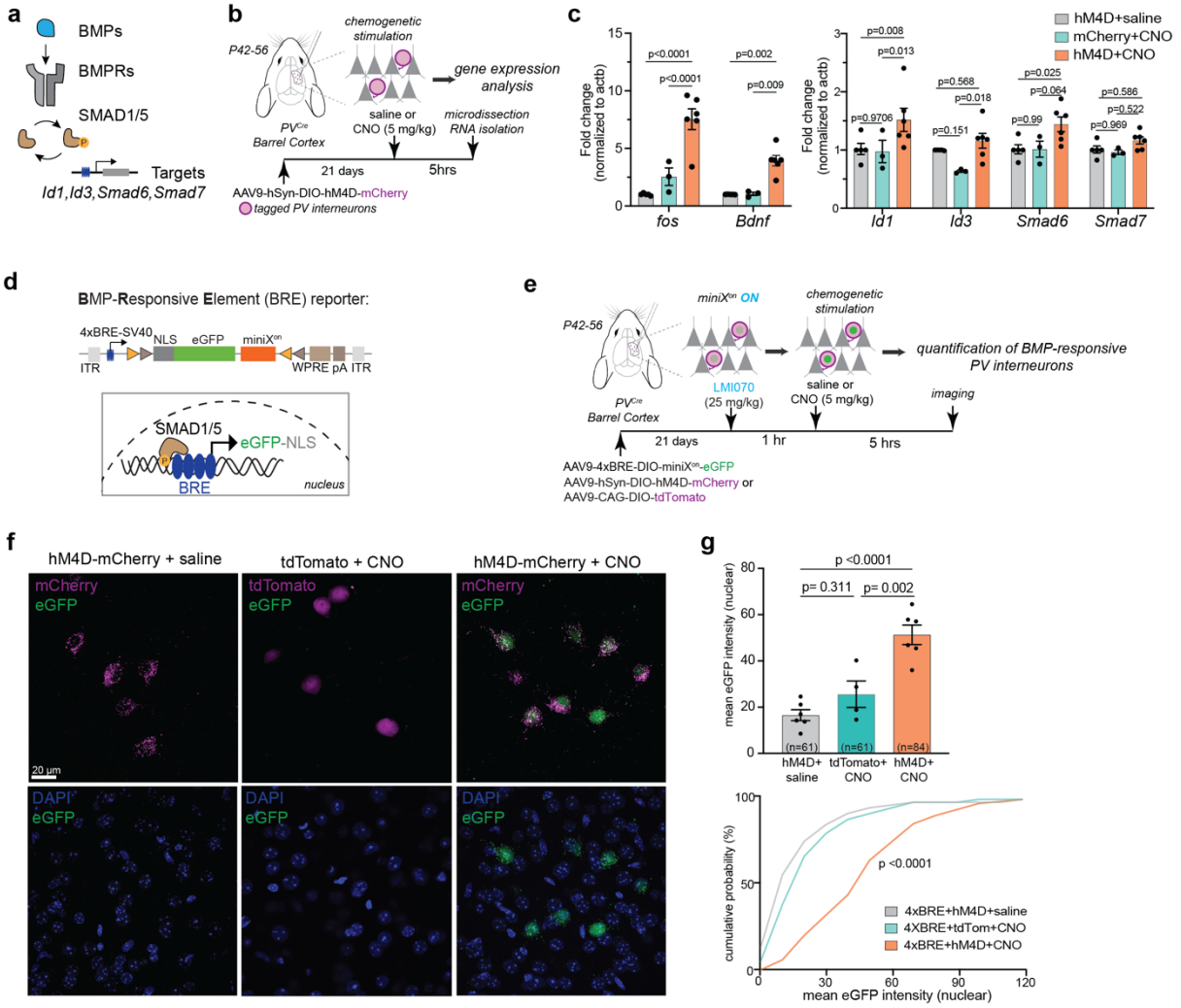

Fig. 1. Neural activity elevation elicits BMP signaling in PV interneurons of the adult barrel cortex. (**a**) Illustration of BMP pathway components (adopted from [32]). (**b**) Schematic representation of chemogenetic neuronal activity manipulation protocol in adult barrel cortex. **(c)** Expression of immediate early genes *cFos* and *Bdnf* and SMAD1/5 target genes *Id1*, *Id3*, *Smad6*, and *Smad7* in barrel cortex of chemogenetically stimulated and control mice (N=3-6 mice/group). Two-way ANOVA with Tukey's post hoc test. **(d)** Schematic representation of viral vector for expression of nuclear eGFP reporter (NLS-eGFP) under control of BMP reporter element (4xBRE) and the miniX^{on} splicing cassette. **(e)** Experimental paradigm. **(f)** Representative images of 4xBRE-driven eGFP signal in the nucleus of layer 2/3 PV interneurons marked by cre-dependent expression of hM4Di-mCherry or tdTomato, respectively. **(g)** Quantification of BRE signaling reporter readout in chemogenetically stimulated and control PV interneurons. Bar graph for mean ± SEM of nuclear eGFP intensity per mouse (N=4-6 mice/group, n=61-84 cells per condition, Kruskal-Wallis test with Dunn's multiple comparisons) and cumulative distribution of eGFP reporter intensity per PV interneuron (Komolgorov-Smirnov test).

Fig. 2

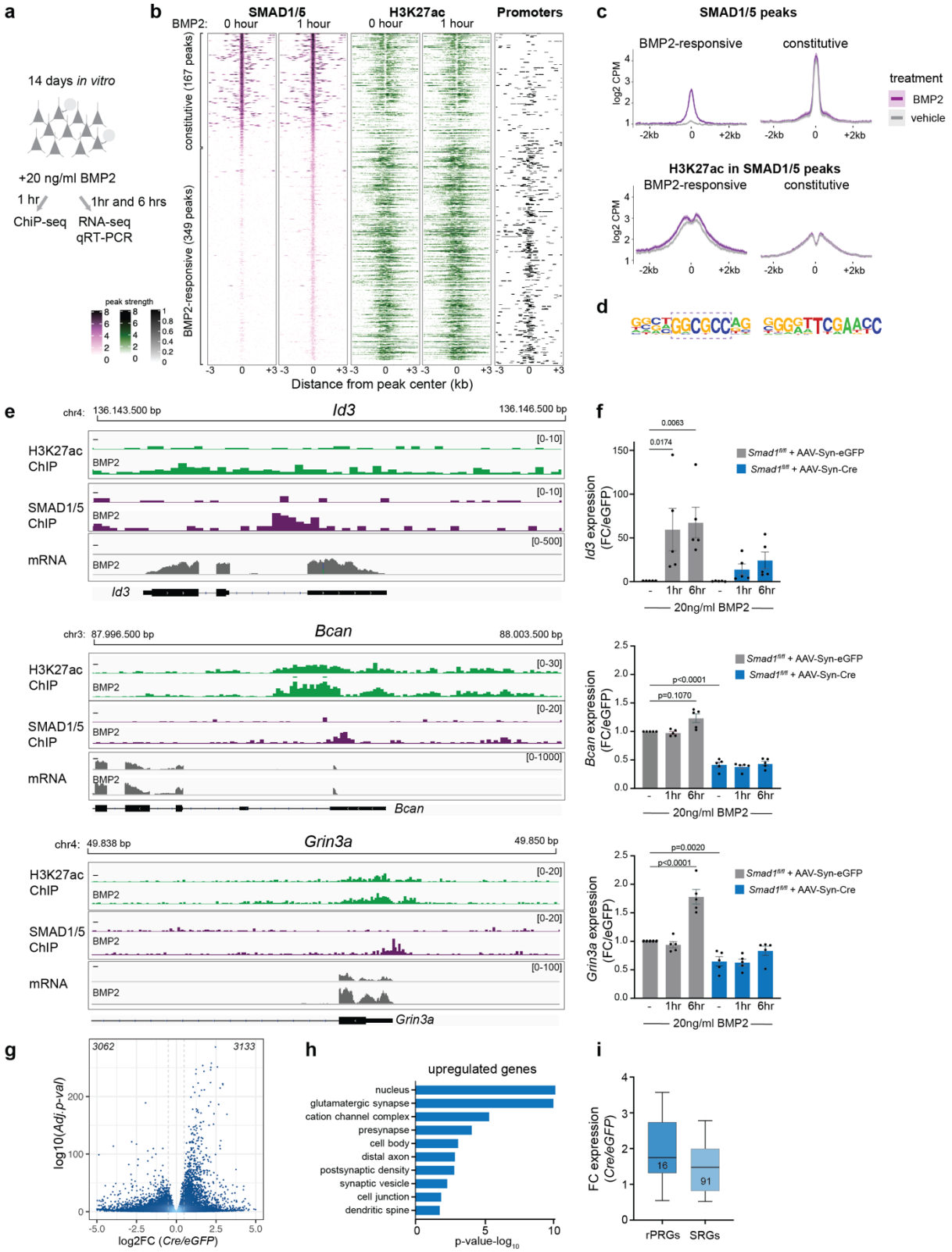

Fig. 2. BMP2-SMAD1 signaling regulates synaptic components and is required for stable cortical networks. (a) Schematic representation of BMP2 stimulation experiments from neocortical cultures. **(b)** ChiP-seq analysis of naïve (0 hour) and growth factor-stimulated (1hour 20ng/ml BMP2) neocortical neuron cultures at DIV14. Heatmaps in purple display peak strength of SMAD1/5 binding, heatmaps in green show H3K27ac binding at SMAD1/5 peak regions. The right column (in

black) displays position of promoter elements. Each binding site is represented as a single horizontal line centered at the SMAD1/5 peak summit, color intensity correlates with sequencing signal for the indicated factor. Peaks are ordered by decreasing Smad1/5 peak intensity. **(c)** Mean normalized ChiP-seq signal for SMAD1/5 and H3K27ac plotted for BMP2-responsive and constitutive SMAD1/5 binding sites. Gray lines indicate signal obtained from vehicle-treated cultures and purple lines signal obtained from BMP2-stimulated cultures. **(d)** Top enriched motifs detected for BMP2-responsive (left) and constitutive (right) SMAD1/5 peaks. **(e)** Examples of IGV genome browser ChiP-seq tracks displaying H3K27ac (green), SMAD1/5 (purple) and RNA-seq signal for SMAD1/5 targets *Id3*, *Bcan* and *Grin3a* in naïve (-) and BMP2-stimulated cultures. **(f)** qPCR analysis of mRNA expression of *Id3*, *Bcan* and *Grin3a* mRNAs in AAV-Syn-eGFP infected *versus* AAV-Syn-Cre infected *Smad1*$^{fl/fl}$ neocortical cultured neurons. Fold change (FC) relative to unstimulated cells is shown for 1 hour and 6 hours stimulation with 20ng/ml BMP2. **(g)** Vulcano plot of differential gene expression in naïve *Smad1*$^{fl/fl}$ cortical cultures infected with AAV-Syn-iCre infected *versus* AAV-Syn-eGFP. Dashed lines indicate log_2FC:0.4 and -log10Adj.-p-val: 2 chosen as thresholds for significant regulation. Number of significantly down- and up-regulated genes are indicated on the top. **(h)** Top ten enriched cellular component gene ontology terms for genes upregulated in conditional *Smad1* mutant cells (*Smad1*$^{fl/fl}$ infected with AAV-Syn-iCre) in unstimulated cortical cultures. **(i)** Expression levels of neuronal activity-regulated rapid Primary Response Genes (rPRGs) and Secondary Response Genes (SRGs) as defined in [56] in conditional *Smad1* mutant cells (*Smad1*$^{fl/fl}$ infected with AAV-Syn-iCre) compared to control AAV-Syn-eGFP infected cultures. The bar graphs show the means ± SEM (N=5 per condition, one-way ANOVA with Dunnett's multiple comparisons).

Fig. 3

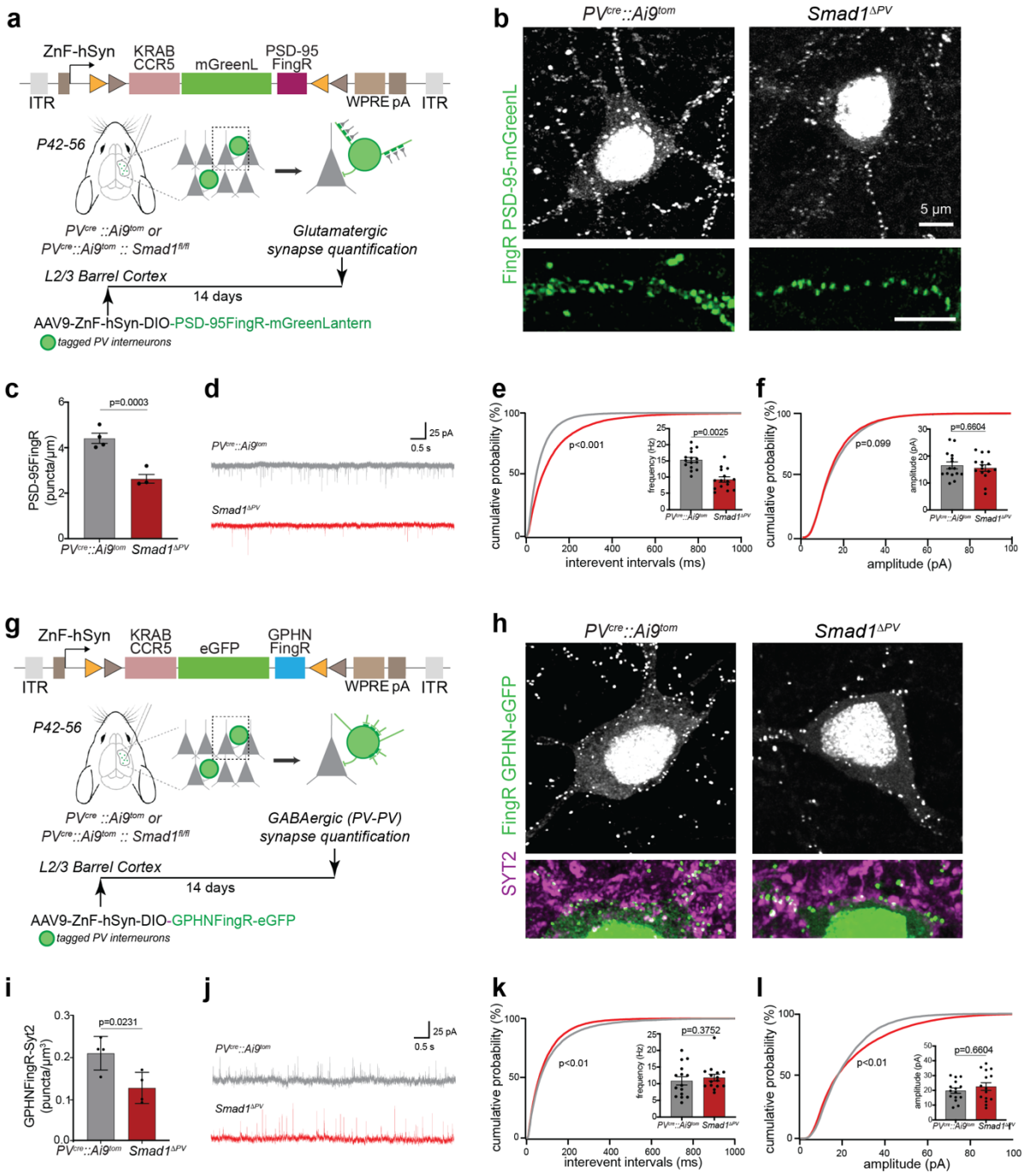

Fig. 3. SMAD1 regulates glutamatergic innervation of PV interneurons. (a) Schematic representation of AAV-driven, cre-recombinase-dependent intrabody probes for glutamatergic (PSD-95FingR-mGreenL) synapses. Intrabody expression is driven from human synapsin promoter (hSyn) fused to a CCR5 zinc finger binding site (ZnF). Intrabody coding sequences (FingRs) are fused to mGreenLantern and a CCR5-KRAB transcriptional repressor for autoregulation of probe expression. Thus, excess probe accumulates in the nucleus. **(b)** FingRPSD-95mGreenLantern-marked synapses formed onto control (*PV^{cre}::Ai9^{tom}*) and *Smad1* conditional knock-out (*Smad1$^{\Delta PV}$*) PV interneurons and corresponding dendritic stretches. **(c)** Quantification of glutamatergic synapse density on the dendrites of PV interneurons. Number of synapses was normalized to dendritic length (Mean and SEM from N=3-4 animals per genotype, n=40 cells per genotype, unpaired t-test). Note that the vast majority of PSD-95FingR-mGreenLantern-marked structures co-localize with the presynaptic marker vGluT1 (see FigS6A). **(d)** Representative traces of mEPSC recordings from

control (gray) and *Smad1*$^{\Delta PV}$ (red) PV interneurons in acute slice preparations from adult mice. **(e)** Frequency distribution of interevent intervals (Kolmogorov-Smirnov test) and mean mEPSC frequency (mean ± SEM for n=15 cells/genotype, from N=4 mice. Kolmogorov-Smirnov test). **(f)** Frequency distribution of mEPSC amplitudes (Kolmogorov-Smirnov test) and mean mEPSC amplitude (mean ± SEM for n=15 cells/genotype, from N=4 mice. Kolmogorov-Smirnov test). **(g)** Schematic representation of AAV-driven, cre-recombinase-dependent intrabody probes for GABAergic (GPHNFingR-eGFP) synapses, fused to eGFP and a CCR5-KRAB transcriptional repressor for autoregulation of probe expression. Thus, excess probe accumulates in the nucleus. **(h)** Synapses formed onto control (*PV*^{cre}*::Ai9*^{tom}) and *Smad1* conditional knock-out (*Smad1*$^{\Delta PV}$) PV interneurons. **(i)** Quantification of PV-PV GABAergic synapse density on PV interneuron somata. Number of GPHNFingR-eGFP / Synaptotagmin2 (SYT2) – containing structures was normalized to soma volume (mean and SEM from N=3-4 animals per genotype, n=78 cells, unpaired t-test). **(j)** Representative traces of mIPSCs recorded from control (in gray) and *Smad1*$^{\Delta PV}$ (red) PV interneurons in acute slice preparations. **(k)** Frequency distribution of interevent intervals (Kolmogorov-Smirnov test) and mean mIPSC frequency (mean ± SEM for n=15 cells/genotype, from N=4 mice. Kolmogorov-Smirnov test). **(l)** Frequency distribution of mIPSC amplitudes (Kolmogorov-Smirnov test) and mean mIPSC amplitude (mean ± SEM for n=15 cells/genotype, from N=4 mice. Kolmogorov-Smirnov test).

Fig. 4

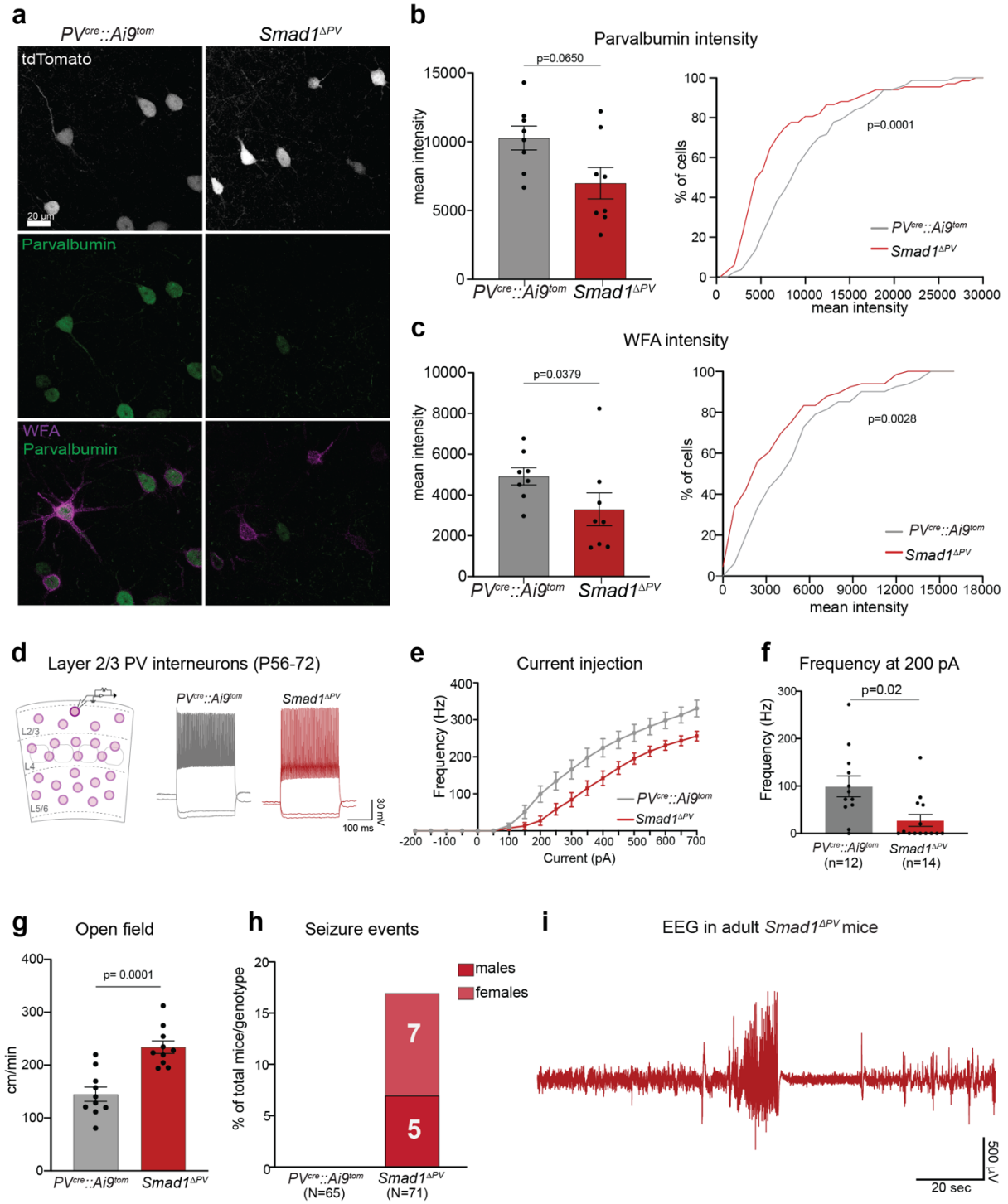

Fig. 4. Loss of SMAD1 in PV interneurons results in disruption of E/I balance in the adult mice. (a) Parvalbumin immunoreactivity and Wisteria floribunda agglutinin (WFA)-binding to the PNNs in adult control (*PV^{cre}::Ai9^{tom}*) and *Smad1* conditional knock-out (*Smad1$^{\Delta PV}$*) mice. **(b)** Quantification of parvalbumin immunoreactivity per cell in *PV^{cre}::Ai9^{tom}* (gray) and *Smad1$^{\Delta PV}$* (red) mice. Bar graphs with mean intensity per mouse (N=8/genotype) and cumulative distribution of mean intensity per cell (n=81 cells for *PV^{cre}::Ai9^{tom}*, n=67 cells for *Smad1$^{\Delta PV}$* mice). Kolmogorov-Smirnov test for bar graph and cumulative distribution). **(c)** As in B but plotting WFA staining intensity. **(d)** Experimental strategy and example traces from current-clamp recordings of control (in gray) and *Smad1$^{\Delta PV}$* (red) PV interneurons in acute slice preparations. **(e)** Comparison of firing

frequencies of layer 2/3 PV interneurons at given currents and **(f)** Mean firing frequency in response to 200 pA current injection in cells from *PV*^{cre}*::Ai9*^{tom} (gray) and *Smad1*$^{\Delta PV}$ (red) mice (N=4 mice, n=12 cells for *PV*^{cre}*::Ai9*^{tom} and N=4, n=14 cells for *Smad1*$^{\Delta PV}$, Kolmogorov-Smirnov test). **(g)** Quantification of the velocity in open field from adult *PV*^{cre}*::Ai9*^{tom} (gray) and *Smad1*$^{\Delta PV}$ (red) mice (N=10 mice/genotype, unpaired t-test). **(h)** Number of *PV*^{cre}*::Ai9*^{tom} control (0 out of 65 mice) and male and female *Smad1*$^{\Delta PV}$ (red) mice (12 out of 71 mice) displaying spontaneous seizures during cage changes. **(i)** Representative 2.5 minutes EEG trace obtained from a *Smad1*$^{\Delta PV}$ mouse. All bar graphs show the means ± SEM.